Novel *PDGFRB* rearrangement in multifocal infantile myofibromatosis is tumorigenic and sensitive to imatinib

Mohammed Hassan,[1] Erin Butler,[1,3] Raphael Wilson,[1] Angshumoy Roy,[4] Yanbin Zheng,[1] Priscilla Liem,[1] Dinesh Rakheja,[5] Dean Pavlick,[6] Lauren L. Young,[6,7] Mark Rosenzweig,[6] Rachel Erlich,[6] Siraj M. Ali,[6] Patrick J. Leavey,[1,2,3] D. Williams Parsons,[4] Stephen X. Skapek,[1,2,3] and Theodore W. Laetsch[1,2,3]

[1]Division of Hematology/Oncology, Departments of Pediatrics, [2]Harold C. Simmons Comprehensive Cancer Center, University of Texas Southwestern Medical Center, Dallas, Texas 75390, USA; [3]Pauline Allen Gill Center for Cancer and Blood Disorders, Children's Health, Dallas, Texas 75235, USA; [4]Baylor College of Medicine, Houston, Texas 77030, USA; [5]Department of Pathology, University of Texas Southwestern Medical Center, Dallas, Texas 75390, USA; [6]Foundation Medicine, Inc, Cambridge, Massachusetts 02141, USA; [7]Beam Therapeutics, Cambridge, Massachusetts 02139, USA

Abstract Infantile myofibromatosis (IM) is an aggressive neoplasm composed of myofibroblast-like cells in children. Although typically localized, it can also present as multifocal disease, which represents a challenge for effective treatment. IM has previously been linked to activating somatic and germline point mutations in the PDGFRβ tyrosine kinase encoded by the *PDGFRB* gene. Clinical panel-based targeted tumor sequencing of a tumor from a newborn with multifocal IM revealed a novel *PDGFRB* rearrangement, which was reported as being of unclear significance. Additional sequencing of cDNA from tumor and germline DNA confirmed a complex somatic/mosaic *PDGFRB* rearrangement with an apparent partial tandem duplication disrupting the juxtamembrane domain. Ectopic expression of cDNA encoding the mutant form of PDGFRB markedly enhanced cell proliferation of mouse embryo fibroblasts (MEFs) compared to wild-type PDGFRB and conferred tumor-forming capacity on nontumorigenic 10T1/2 fibroblasts. The mutated protein enhanced MAPK activation and retained sensitivity to the PDGFRβ inhibitor imatinib. Our findings reveal a new mechanism by which PDGFRB can be activated in IM, suggest that therapy with tyrosine kinase inhibitors including imatinib may be beneficial, and raise the possibility that this receptor tyrosine kinase might be altered in a similar fashion in additional cases that would similarly present annotation challenges in clinical DNA sequencing analysis pipelines.

Corresponding author:
ted.laetsch@utsouthwestern.edu

Ontology term: neoplasm of the skin

[Supplemental material is available for this article.]

INTRODUCTION

Infantile myofibroma is a relatively rare form of soft tissue neoplasm that is primarily diagnosed in children of <12 mo of age (Parham 2018). The multifocal disease is known as infantile myofibromatosis (IM), which if untreated carries a mortality rate of 70% when lesions are present in viscera (Wiswell et al. 1988; Day et al. 2002; Mashiah et al. 2014; Weaver et al. 2015; Wu et al. 2015). Historically, treatment for myofibromatosis ranges from expectant management or surgical resection alone to the application of systemic, low-dose chemotherapy for those with multifocal or unresectable disease (Azzam et al. 2009; Mashiah et al. 2014; Weaver et al. 2015; Parham 2018). This neoplasm also presents with circumscribed lesions

with histologic appearance of spindled cells and immunohistochemical staining patterns that demonstrate similarities between IM and infantile fibrosarcoma (Alaggio et al. 2008; Parham 2018).

Molecular genetic studies have recently identified activating mutations in platelet-derived growth factor β (PDGFRβ) in most IM cases. PDGFRβ is a transmembrane receptor tyrosine kinase encoded by the *PDGFRB* gene (Forsberg et al. 1993; Hellström et al. 1999; Hoch and Soriano 2003; Tallquist and Kazlauskas 2004; Andrae et al. 2008). The *PDGFRB* gene is primarily expressed in cells of mesenchymal origin, including smooth muscle cells, and analyses of genetically engineered mouse models show *PDGFR* to be essential for embryonic development in part by controlling perivascular cell accumulation/localization (Soriano 1994; Hoch and Soriano 2003). The PDGF signaling pathway has long been recognized to play a critical role in propelling the cell division cycle from G_1 phase into S phase (Pardee 1989). Deregulated activation of PDGFRβ has been identified in human cancers, including by a rearrangement-generated fusion protein, originally described in a child with chronic myelomonocytic leukemia that harbored a TEL-PDGFR fusion (Golub et al. 1994) and subsequently in *RABEP1-PDGFRB* and *CEV14-PDGFRB* fusions in myelogenous leukemia (Abe et al. 1997; Magnusson et al. 2001). PDGFRβ is also activated by autocrine/paracrine stimulation through increased expression of its ligand, PDGF-B, exemplified by the *COL1A1-PDGFB* translocation in dermatofibrosarcoma protuberans (Wang et al. 1999; McArthur 2006). Few human cancers have been described to harbor kinase-activating *PDGFRB* mutations, with the exception of IM, in which both somatic and germline missense mutations in *PDGFRB* have been identified (Cheung et al. 2013; Martignetti et al. 2013; Agaimy et al. 2017; Arts et al. 2017; Murray et al. 2017; Pond et al. 2018). Germline *PDGFRB* gain-of-function mutations appear to underlie the majority of familial cases (eight of nine unrelated families in one series) (Martignetti et al. 2013), and a substantial fraction of patients with sporadic multifocal disease have either germline, somatic, or mosaic gain-of-function mutations (Arts et al. 2017). The majority of the *PDGFRB* mutations described to date in IM alter the juxtamembrane domain, defeating an auto-inhibitory feedback loop, or alter the kinase domain, presumably resulting in constitutive activation (Agaimy et al. 2017; Arts et al. 2017).

In this article, we present the case of a newborn child with seemingly sporadic, multifocal IM. Clinical molecular genetic analysis of the tumor revealed a novel *PDFGRB* rearrangement initially reported as a variant of unknown clinical significance. Additional molecular genetic analyses and in vitro functional studies demonstrate the oncogenic activity of this newly recognized mutant allele. To our knowledge, this is the first case of a rearrangement in *PDFGRB* reported in IM and represents a novel mechanism of PDGFRβ activation in this disease.

RESULTS

Clinical Case Presentation

A 9-day-old African–American girl presented to the pediatric surgery team for evaluation of a well-circumscribed, nontender, and firm soft tissue mass on the anterior abdominal wall. The mass was noted at birth but was undetected on prenatal ultrasound evaluations. Similar subcutaneous nodules were also noted on the upper back and left hip. The full-term child, born after an unremarkable prenatal course, was in otherwise good health. An abdominal ultrasound on day of life 1 showed the left upper quadrant soft tissue mass to measure 1.9 cm × 1.2 cm × 2.7 cm and confirmed its location in the subcutaneous tissue. A small focus of vascular flow was thought to be consistent with a hemangioma or congenital vascular anomaly. Following a period of observation, abdominal MRI at ~2 mo of age revealed multiple, rim-enhancing lesions within the abdomen and pelvis (Fig. 1A). These included both osseous
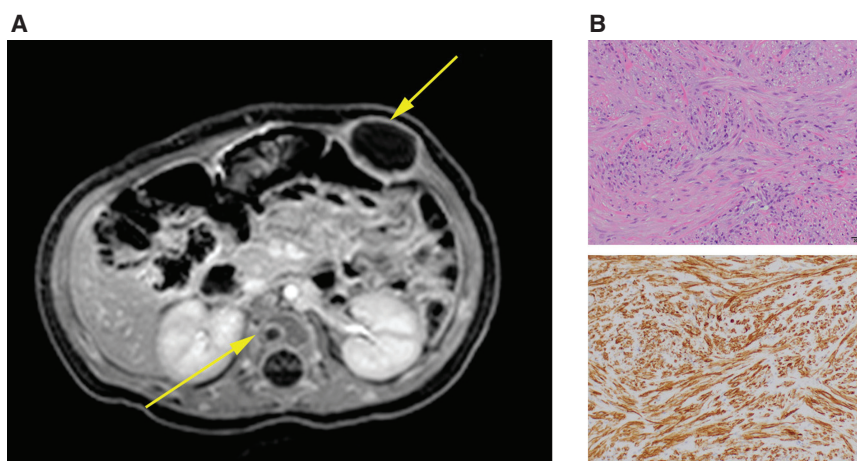
Figure 1. Tumor analysis and classification. (*A*) Postcontrast T1-weighted MRI demonstrates multiple rim-enhancing masses in the abdominal wall musculature and vertebral body. (*B*) Histopathologic examination of a biopsy from the abdominal wall mass shows a myofibroma. (*Top*) Hematoxylin and eosin, 200× magnification: (*bottom*) smooth muscle actin immunostain, 200× magnification.

and muscular lesions and one within the pancreatic head. An additional 10-mm lesion was noted in the left ventricular free wall on echocardiogram. The radiographic differential diagnosis of these lesions included infection, neurofibroma, multifocal Langerhans cell histiocytosis, metastatic neuroblastoma, and IM.

The child underwent an incisional biopsy of the left upper quadrant subcutaneous lesion, which had remained unchanged in appearance since birth. Intraoperatively, the mass was noted to be cystic and fused to the anterior abdominal wall, which prevented a complete excision without excessive morbidity. Gross pathologic analysis revealed a tan-pink to tan-white, firm, rubbery mass. Light microscopy revealed bland, medium-sized, round to spindled cells with vacuolated nuclei arranged in a fascicular pattern and rare mitotic figures in a collagenous fibromyxoid stromal background. Immunohistochemical stains were performed, and the tumor stained positive for β-catenin (cytoplasmic only) and smooth muscle actin (Fig. 1B; and data not shown). These pathology studies and the clinical presentation were sufficient to make a diagnosis of IM. The child was treated with vinblastine and methotrexate chemotherapy and had a stable disease at 13 mo of age, after 9 mo of therapy. The child has since been lost to follow-up. Whether vinblastine/methotrexate contributed to the disease stabilization is not clear.

Molecular Genetic Analyses

Formalin-fixed, paraffin-embedded tissue samples from the diagnostic specimen were analyzed using FoundationOne Heme, a commercial hybrid capture-based next-generation sequencing (NGS) assay. Sequencing revealed a *CDKN2A* missense variant predicted to influence the amino acid sequence of p14^{ARF} (S73R) but not p16^{INK4A} (R58R) and a rearrangement of *PDGFRB* reported as a variant of uncertain significance (Table 1). As the significance of p14$^{ARF-S73R}$ is uncertain (di Tommaso et al. 2009), we chose to focus on the *PDGFRB* rearrangement. Further manual review of the NGS data for *PDGFRB* suggested a complicated deletion/duplication in which 13 nt are deleted from within exon 12 (breakpoints Chr 5: 149,505,080, Chr 5:149,505,067) and replaced by a duplicated portion of intron 14 and exon 15 (breakpoints intron 14—Chr 5: 149,502,780, exon 15—Chr 5: 149,502,629) (Fig. 2A,B). Sanger sequencing of segments of genomic DNA and cDNA

Table 1. Variant table

Gene	Chromosome	HGVS DNA reference	HGVS protein reference	Variant type	Predicted effect (substitution, deletion, etc.)	dbSNP/ dbVar ID	Genotype (heterozygous/ homozygous)
PDGFRB	Chr 5	NM_002609:c.1736_2024-17del1747_2160dup	NP_002600.1: P.LYS559ASPFSTER569	Insertion/ deletion	Frameshift	N/A	Heterozygous
CDKN2A	Chr 9	NM_058195:c.217A>C NM_000077:c.174A>C NM_001195132: c.174A>C NM_058197:c.*97A>C	NP_478102.2:p.Ser73Arg NP_000068.1:p.Arg58= NP_001182061.1: p.Arg58=	Single-nucleotide variant	Substitution/ synonymous/UTR	rs201208890	Heterozygous

amplified by PCR confirmed the presence of this rearrangement in tumor which was not identified in germline DNA obtained from peripheral blood mononuclear cells suggesting a somatic or germline mosaic event not affecting hematopoietic precursors (Supplemental Fig. 2). On the mRNA level, the 5′ end of exon 12, joined to an intronic sequence from intron 14 and lacking the 3′ splice donor site, is spliced out of the transcript, resulting in a net replacement of 73 nt of exon 12 of the *PDGFRB* transcript by 136 nt of *PDGFRB* exon 15
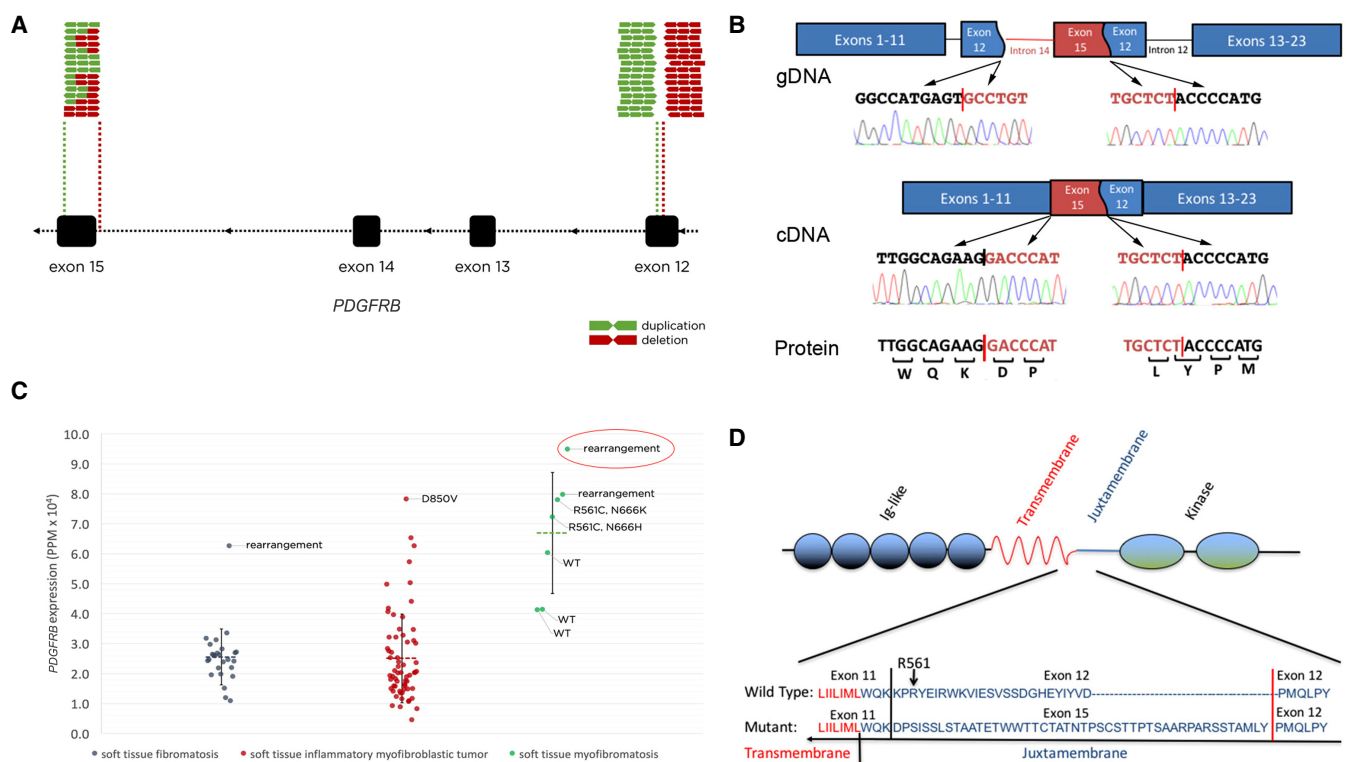

Figure 2. Sequencing and mapping of the gene rearrangement. (*A*) Complex *PDGFRB* rearrangement is detected by next-generation sequencing (NGS). The rearrangement was detected in DNA and RNA by NGS but is difficult to ascertain because of event complexity. (*B*) *PDGFRB* rearrangement predicted by NGS is confirmed by Sanger sequencing of genomic DNA (gDNA) and RNA (cDNA) from tumor. (*C*) *PDGFRB* is highly expressed in RNA-seq data from the patient's tumor (circled) compared to other cases of IM with and without activating *PDGFRB* point mutations. (*D*) Rearrangement results in the replacement of a portion of the juxtamembrane domain of PDGFRβ by a novel amino acid sequence derived from a portion of exon 15 read out-of-frame. The wild-type kinase domain is retained.

(Fig. 2D). In the resulting putative PDGFRβ protein, 25 amino acids of the auto-inhibitory juxtamembrane domain are replaced by 46 amino acids generated by reading exon 15 of *PDGFRB* out-of-frame. The predicted amino acid sequence reverts to the wild-type reading frame at the junction between exons 15 and 12; hence, the kinase domain is intact and remains in-frame. Notably, this alteration eliminates a portion of the juxtamembrane domain, including the arginine residue at position 561, which has been reported to form a salt bridge that tethers the auto-inhibitory juxtamembrane domain to the kinase domain, facilitating inhibition of kinase activity (Toffalini and Demoulin 2010). Interestingly, normalized *PDGFRB* mRNA expression in this tumor (IM-P^{ITD}) was higher than the PDGFRB expression in three analyzed IM cases lacking PDGFRB alterations (IM-P^{wt}), two IM cases harboring PDGFRB missense mutations but no rearrangements (IM-P^{mut}), and any of the analyzed fibromatosis (FM) or inflammatory myofibroblastic tumor (IMT) cases in the Foundation Medicine database (Fig. 2C). Although our mRNA expression analysis did not distinguish between the mutant and wild-type transcripts, taken together, our findings suggest this IM tumor harbors a pathogenic *PDGFRB* complex rearrangement accompanied by high levels of *PDGFRB* mRNA expression, suggesting that *PDGFRB* activation is an oncogenic driver in this IM tumor.

Functional Analyses of the Mutant *PDGFRB* Variant

We generated lentiviral expression vectors driving expression of GFP only (CTL) or GFP and either PDGFRβ (P-WT) or the PDGFRβ-ΔEx12 mutant cDNA identified in this patient (P-Ex12); vectors expressing GFP only served as a control. Following transduction of MEFs derived from *Pdgfrb*$^{-/-}$ mice at a MOI of 1, we used RT-PCR and western blotting to show expression of each form (Fig. 3A–C) and found higher levels of phospho-p44/p42 MAPK in cells transduced by P-Ex12 than in cells transduced by P-WT, despite lower levels of PDGFRβ protein in P-Ex12 transduced cells (Fig. 3C). We studied the impact of their expression on the capacity of the MEFs to form colonies when cultivated at low density on tissue culture plates. After 14 d, those assays showed that cells expressing P-Ex12 had increased colony formation compared with both P-WT and control vector expressing cells (Fig. 3D,E; *t*-test; $P < 0.05$). Consistent with conferring a substantial growth advantage, our capacity to serially propagate *Pdgfrb*$^{-/-}$ MEFs expressing either CTL or PDGFRβ diminished as they approached passage number 7. In contrast, P-Ex12-expressing *Pdgfrb*$^{-/-}$ MEFs continued unabated through passage number 25, at which time we concluded the experiment.

Reasoning that functional advantage of PDGFRβ-ΔEx12 might be exaggerated within a *Pdgfrb*$^{-/-}$ background, we carried out similar experiments using 10T1/2 fibroblasts, a well-characterized fibroblast line originally derived from C3H mouse embryos (Reznikoff et al. 1973); the line has biallelic deletion of the *Cdkn2a* gene (SX Skapek, unpubl.), an event recognized to frequently occur in immortalized mouse fibroblasts (Kamijo et al. 1997). Using primers that amplify both mouse and human forms of *PDGFRB* cDNA, RT-PCR showed the expression of endogenous as well as the ectopic transcripts (Fig. 4A). Western blotting for PDGFRβ showed increased expression of the receptor in transduced cells with the level being approximately equal for wild-type PDGFRβ and P-Ex12, detected at 14 d following transduction (Fig. 4B). Western blotting also showed phospho-p44/p42 MAPK, known to be enhanced by PDGFRβ signaling (Andrae et al. 2008), was increased in cells with ectopic PDGFRβ, with higher levels of phosphorylation seen in cells transduced by P-Ex12 than in cells transduced by P-WT, despite the latter exhibiting higher levels of total PDGFRβ protein (Fig. 4B).

Despite increased phospho-p44/p42 MAPK in P-Ex12-transduced 10T1/2 cells, we could not detect increased cell accumulation in the low-density plating assay, perhaps because the cells are already immortalized because of biallelic *Cdkn2* deletion (MH and SXS; negative data not shown). Nevertheless, we tested whether P-Ex12 might confer tumor-forming capacity by implanting cells transduced with control lentiviral vectors or vectors
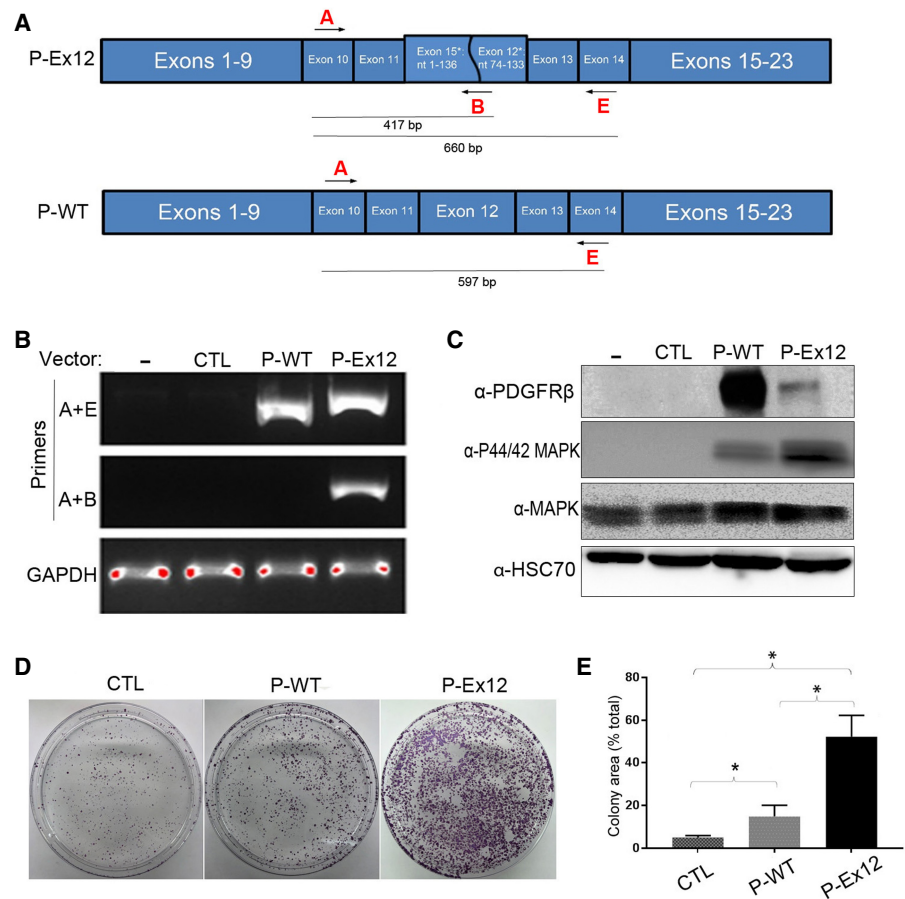
Figure 3. Functional evaluation of the rearrangement using *PDGFRB*-null mouse embryonic fibroblasts. (*A*) Diagram shows primers amplification for both wild-type *PDGFRB* (WT) and *PDGFRB* bearing the rearrangement identified in this patient's tumor (P-Ex12). (*B*) RT-PCR of *PDGFRB*–null mouse embryonic fibroblasts (MEFs) transduced with lentivirus expressing GFP only (CTL), P-WT, or P-Ex12. (*C*) A representative western blot of *PDGFRB*–null mouse embryonic fibroblasts that demonstrates expression of *PDGFRB* in P-WT- and P-Ex12-transduced cells and increased expression of phospho–p44/42 MAPK of cells transduced with P-Ex12 as compared to P-WT- and CTL-expressing mouse embryonic fibroblasts. (*D*) Photographs of colony formation assay of MEFs plated at low density show increased colony formation in P-Ex12-expressing cells compared to P-WT- and CTL-expressing MEFS. (*E*) Quantification of cell plate area covered by transduced MEFS shown in *D*.

expressing wild-type (P-WT) or mutant forms of PDGFRβ (P-Ex12) into NOD-SCID mice. In two separate experiments involving a total of five animals per group, no tumor growth was evident in 10 total mice carrying CTL or P-WT cells through 80 total days of follow-up; however, three of five animals implanted with P-Ex12-expressing cells formed tumors that reached maximum acceptable size between 28 and 75 d postimplantation (Fig. 4C). One additional animal in that cohort died without obvious tumor formation, and the carcass was removed before necropsy was performed. Whether the biallelic *Cdkn2a* deletion contributed to the tumor-forming capacity in the P-Ex12-expressing 10T1/2 cells is not known.

Histological analysis of two of the P-Ex12-driven tumors demonstrated a high-grade neoplasm based on nuclear atypia, frequent and abnormal mitotic figures, evidence for necrosis, and evidence by light microscopy of tumor invasion into neurovascular tissues and adjacent skeletal muscle, resembling a high-grade sarcoma (Fig. 4D). PCR confirmed retention of the
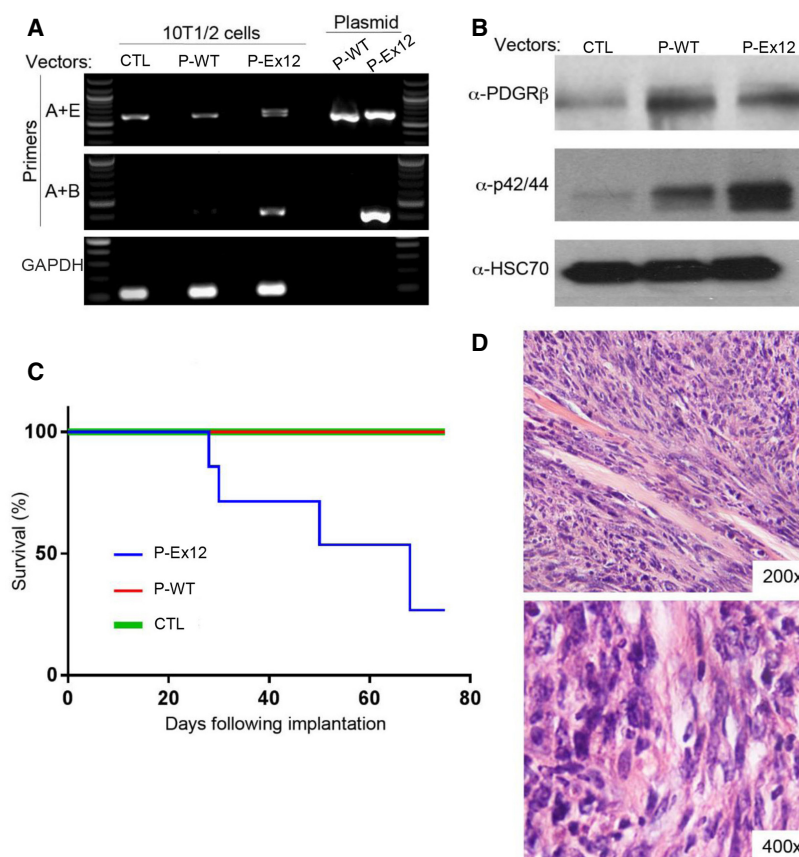
Figure 4. P-Ex12 is tumorigenic in 10T1/2 fibroblasts. (*A*) RT-PCR of 10T1/2 cells transduced with P-Ex12, P-WT, and CTL lentiviral vectors. (*B*) Representative western blot of 10T1/2 cells confirms expression of PDGFRB and increased expression of phospho-p44/42 MAPK of cells transduced with lentivirus bearing P-Ex12 as compared to P-WT- and CTL-expressing fibroblasts. (*C*) Kaplan–Meier plot displays decreased overall survival of mice bearing P-Ex12-transduced 10T1/2 cells compared to both CTL- and P-WT-transduced cells. (*D*) Histopathological examination of processed tumor samples show signs of tumor infiltration through nerve cells, blood vessels, and muscle cells and areas of necrosis (hematoxylin and eosin, 200× and 400× magnification).

P-Ex12 lentiviral vector (Fig. 5A), and immunostaining for both Ki67 and phospho-histone H3 demonstrated high proliferation (Fig. 5B).

Finally, we utilized the colony-forming assay in MEFs transduced with either P-WT- or P-Ex12-expressing vectors to test whether accumulation of the P-Ex12-expressing MEFs could be blunted by imatinib, a potent inhibitor of PDGFRβ and other tyrosine kinases (Arts et al. 2016). Indeed, the P-Ex12-expressing MEFs seemed even more susceptible to imatinib inhibition than MEFs expressing wild-type PDGFRβ (Fig. 6A,B; one-way ANOVA; $P = 0.0002$). In a complementary assay, transduced MEFs cultivated in a 96-well plate showed the IC_{50} for imatinib in P-Ex12-expressing MEFs to be significantly lower than in MEFs expressing wild-type receptor (0.226 μM vs. 1.684 μM, *t*-test; $P = 0.0012$; Fig. 6C). We note that the magnitude of the effect of imatinib on P-Ex12-driven, low-density, colony formation (Fig. 6A,B) seems greater than the effect on P-Ex12-driven cell accumulation (Fig. 6C); this may indicate that P-Ex12 differentially influences those two processes. Because published pharmacokinetic analyses indicate that 1 μM steady state imatinib is well within the levels reached in adult patients treated with standard doses of imatinib (400 mg) (Peng et al. 2004), we
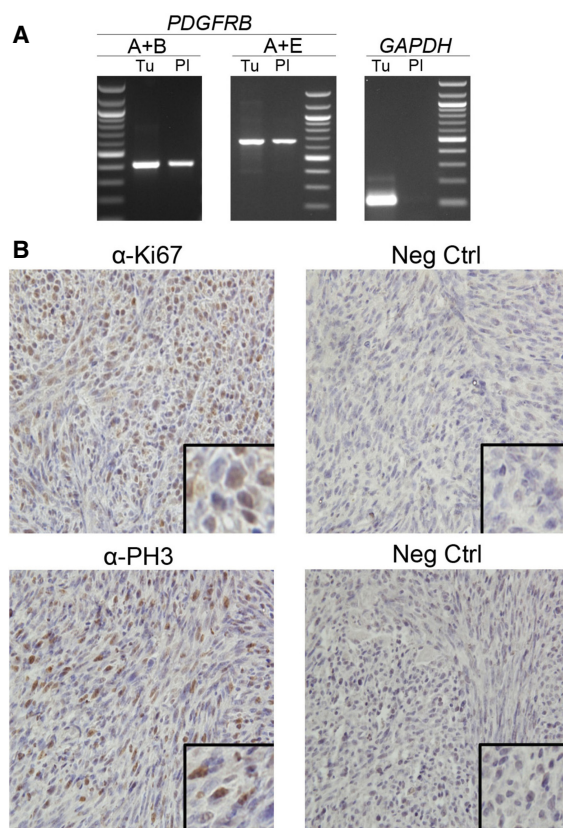
Figure 5. Analysis of tumors formed by 10T1/2 fibroblasts expressing the rearranged PDGFRB cDNA. (*A*) RT-PCR of tumor samples confirms expression of P-Ex12 in the tumor (Tu); plasmid (Pl) used as control in PCR. (*B*) Immunohistochemistry staining of tumor samples shows positive staining for Ki67 (α-Ki67) and phospho-histone H3 (α-PH3).

conclude that expression of the PDGFRβ variant with a disrupted inhibitory juxtamembrane domain represents a vulnerability that can be exploited therapeutically.

DISCUSSION

IM is a relatively rare neoplasm most recently classified by the World Health Organization as a pericytic tumor (Parham 2018), which is consistent with the concept that the tumor can be driven by activating mutations in *PDGFRB*, a gene required for pericyte accumulation in the mouse (Soriano 1994). The clinical presentation and course of IM can range from the presence of a single lesion that regresses spontaneously to multifocal, multiorgan disease which can represent a life-threatening problem (Fukasawa et al. 1994; Mashiah et al. 2014; Parham 2018). For those complex cases, systemic chemotherapy, including the use of vinblastine and methotrexate and other "low dose" cytotoxic agents, has demonstrated activity (Azzam et al. 2009; Weaver et al. 2015). The recognition that most cases of IM are associated with either somatic or germline mutations activating the PDGFRβ kinase has suggested the potential clinical utility of treatment using molecularly targeted agents, such as sunitinib and other kinase inhibitors (Arts et al. 2016; Agaimy et al. 2017; Sramek et al. 2018). It is therefore important to recognize more complicated rearrangements such as that seen in our patient as
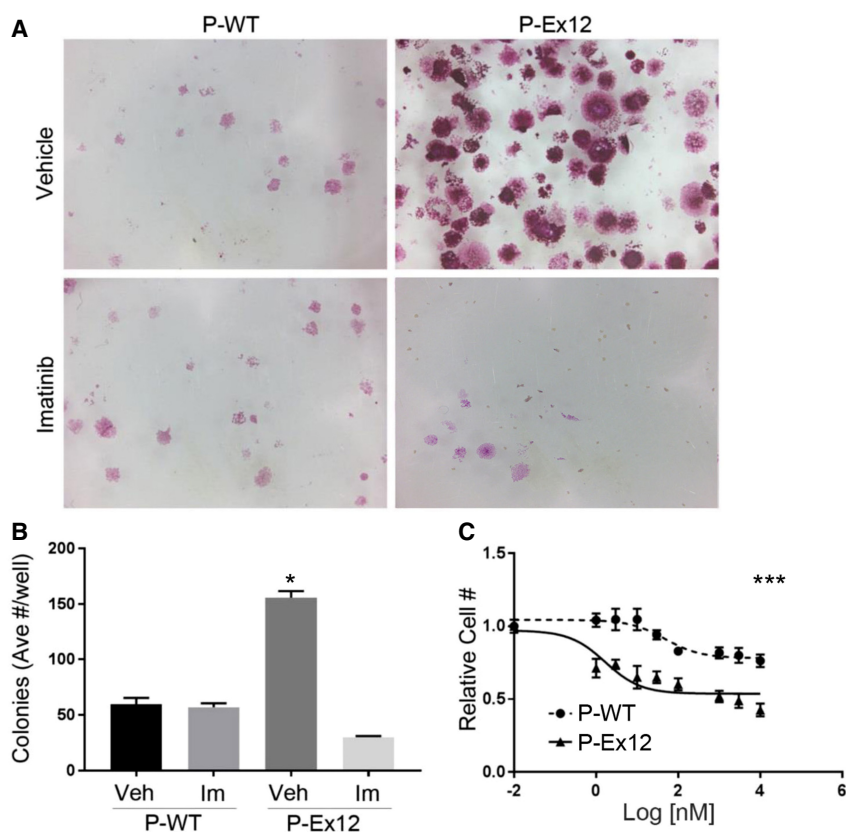
Figure 6. Treatment of transduced mouse embryonic fibroblasts. (*A*) Representative photographs of transduced *PDGFRB*-null mouse embryonic fibroblasts show increased colony formation with P-Ex12 expression that is blunted with imatinib treatment (1 µM). (*B*) Quantification of colony formation in treated and untreated P-WT- and P-Ex12-transduced MEFs. (*C*) MEFs transduced with P-Ex12 demonstrate increased sensitivity to imatinib as compared to P-WT MEFs.

a potential mechanism by which PDGFRβ can be activated and subsequently targeted by molecular therapies. Such rearrangements may be missed by sequencing approaches that only evaluate for targeted hotspot mutations. Moreover, given that *PDGFRB* mutations are common in IM, but rare in infantile fibrosarcoma, which can be histologically similar (Alaggio et al. 2008), the identification of an oncogenic *PDGFRB* alteration may play a role in making the correct diagnosis.

The exact mechanism by which the rearrangement that we describe deregulates PDGFRβ will need to be elucidated in more detail in subsequent studies. However, given the inhibitory nature of the juxtamembrane domain and the presence of activating drug-sensitive alterations disrupting that domain in other receptor tyrosine kinases such as FLT3, PDGFRα, and KIT, it seems likely that disrupting the juxtamembrane domain curtails an auto-inhibitory mechanism leading to the hyperactivation of the kinase domain (Kiyoi et al. 1998, 2002; Chan et al. 2003; Heinrich et al. 2003a,b; Corless et al. 2005; Corbacioglu et al. 2006; Reindl et al. 2006; Stover et al. 2006; Kim et al. 2011; Liang et al. 2016; Short et al. 2019). Previous studies have implicated Arg561 as a key residue for the inhibitory juxtamembrane-kinase domain interaction, and consistent with that model, Arg561 and flanking residues are replaced in the P-Ex12 protein (Fig. 2D; Cheung et al. 2013). Our data show that the P-Ex12 variant activates at least one downstream signaling pathway more robustly than the wild-type protein. Whether the P-Ex12 additionally activates a

different set of signaling pathways than the ligand-stimulated wild-type receptor PDGFRβ, harboring activating mutations, or *PDGFRB* rearrangements such as *TEL-PDGFRB* fusion is not clear at present (Golub et al. 1994). We also noted that the P-Ex12 form was generally found at a lower level than the wild-type protein, when both were ectopically expressed. We suspect that this may be due to differential posttranslational processing, such as ubiquitylation noted to traffic certain RTKs to the lysosome[53], perhaps to help gait excess signaling. The concept needs experimental validation, as does the role of the p14ARF/p16INK4A variants in this case.

An important takeaway from our study is that this new *PDGFRB* variant is not only transforming and able to drive cancer in xenografted mice but is also sensitive to clinical doses of imatinib (Fig. 6), suggesting that this widely available and approved agent can counteract the key PDGFRβ-elicited oncogenic signaling in IM. Similarly, preclinical studies have demonstrated that many of the missense variants in *PDGFRB* which occur in IM are sensitive to inhibition by tyrosine kinase inhibitors, and a recent case report highlights the clinical utility of sunitinib, a PDGFRβ targeting multikinase inhibitor, in a patient with IM with a germline *PDGFRB* p.R561C mutation (Arts et al. 2016, 2017; Mudry et al. 2017). Although we only sequenced a single tumor from this patient, it is likely this represents a mosaic *PDGFRB* rearrangement explaining the patient's multifocal disease. Beyond mutations in *PDGFRB*, the limited number of mutations in other genes associated with IM also suggest that classical IM is a PDGFRβ-driven disease, with alterations of *NOTCH3* predicted to activate PDGFRβ and *PTPRG*, an enzyme that dephosphorylates PDGFRβ also reported in this disease (Martignetti et al. 2013; Linhares et al. 2014). The contribution of the *CDKN2A* variant to this child's disease or IM pathogenesis merits further exploration. Given the remarkable success of tropomyosin receptor kinase (TRK) inhibition for infantile fibrosarcoma (Laetsch et al. 2018), a disease histologically similar to IM and caused by activating fusions in the neurotrophic tyrosine kinase receptor (NTRK) family of genes, a clinical trial of PDGFRβ inhibition in patients with IM is warranted.

METHODS

Pathology and Molecular Analyses of Tumor Specimen

Routine histology processing and diagnostic studies were performed at Children's Health Children's Medical Center Dallas. Unstained formalin-fixed, paraffin-embedded (FFPE) tissue sections were analyzed using the Foundation One Heme panel (Foundation Medicine). In addition, RNA and DNA were extracted from fresh frozen tumor tissue using the AllPrep DNA/RNA Mini Kit (QIAGEN), according to the manufacturer's specifications. PCR and RT-PCR were carried out as previously described (Widau et al. 2012), using primers designed to amplify wild-type and mutated versions of human *PDGFRB* (Supplemental Table 1). The reactions were tested using gDNA and cDNA from U2OS and H290 cell lines, which express *PDGFRB* (Supplemental Fig. 1). PCR and RT-PCR products were run on a 0.8% agarose gel, purified using the QIAGEN QIAquick Gel Extraction Kit, and sequenced at the UTSW McDermott Sequencing Core. Sequencing was completed using Foundation One Heme panel (Foundation Medicine). The sequencing depth for the CDKN2A variant was 651× and the PDGFRB variant is shown in Table 2.

Generating Lentiviral Vectors Expressing Either Wild-Type or Rearranged PDGFRβ

The rearranged *PDGFRB* cDNA amplified from the tumor specimen was digested using *FspI* and *SacII* and subcloned into *pDONR221-hPDGFRB-WT*, a Gateway entry clone containing

Table 2. Sequencing coverage

	Breakpoint #1	Breakpoint #2
Duplication	825×	863×
Deletion	797×	991×

the human *PDGFRB* cDNA (Harvard PlasmID Repository), to generate pDONR221-hPDGFRB-ΔEx12. The cDNA encoding either P-WT and P-Ex12 was subcloned into the pLenti7.3 V5-DEST (Invitrogen) Gateway destination vector by LR recombination to produce lentiviral expression vectors in which CMV promoter drove expression of either P-WT or P-Ex12 as well as EmGFP, driven by the SV40 promoter (pLenti 7.3-hPDGFRB-WT and pLenti 7.3-hPDGFRB-ΔEx12). Note that control vectors expressed only EmGFP. Plasmids were verified at each step of the process by PCR, restriction enzyme digestion, and bidirectional Sanger sequencing.

Lentiviral vector stocks were produced in HEK-293T cells using psPAX2 and pMD2.G packaging and envelope-expressing plasmids (Addgene). Cell culture supernatant was harvested after 48 h, filtered using a 0.45 μm filter, and stored in aliquots at −80°C. A lentiviral titer analysis was completed using 10-fold dilutions and analyzed for fluorescence by FACS analysis. Cells were subsequently transduced at a MOI of 1 and sorted by FACS analysis for GFP expression for functional experiments.

Cell Culture

Mouse embryonic fibroblasts (MEFs) were derived from $Pdgfrb^{-/-}$ embryos harvested at embryonic day (E) 13.5 as products from mating heterozygous mice (Charles River Laboratories). Primary and subcultured MEFs were cultivated as previously described (Silva et al. 2005).

To assess colony-forming capacity, $Pdgfrb^{-/-}$ MEFs transduced to express CTL; P-WT and P-Ex12 were plated (1×10^4 cells/100 mm plate or 2×10^3/well of six-well plate) and cultivated for 14 d. In some cases, cells were treated with of imatinib 1 μM in DMSO (STI571 Catalog No. S2475) or an equivalent volume of DMSO as control. Cells were then fixed using 2% paraformaldehyde and stained with 0.05% crystal violet; photomicrographs were analyze using ImageJ or manual counting.

Functional Evaluations

Ectopic mRNA and Protein Expression

$Pdgfrb^{-/-}$ MEFs or 10T1/2 fibroblasts were transduced, sorted by FACS analysis for GFP expression, and replated onto standard cell culture plates. Expression of P-WT and P-Ex12 was assessed by qRT-PCR or western blotting, essentially as previously described (Silva et al. 2005). RT-PCR primers were designed using the National Library of Medicine PRIMER-BLAST tool, and obtained from Sigma-Aldrich. For western blotting, proteins were solubilized in RIPA lysis buffer supplemented with PhosStop Phosphotase inhibitor and Roche Complete Protease inhibitor (Roche). Primary antibodies recognized human and mouse PDGFRB (EMD Millipore, #04-825), phospho-p42/44 (Cell signaling #9102), total MAPK (Cell Signaling, 9102S), and HSC-70 (Santa Cruz SC-729). Secondary antibodies included anti-goat (Jackson ImmunoResearch 705-035-003), anti-rabbit (Jackson ImmunoResearch 111-035-003), and anti-mouse (Jackson ImmunoResearch 715-035-0150, and protein expression was detected by using both CareStream film (Sigma-Aldrich Z3730398) and Bio-Rad Clarity Enhanced Chemiluminescence (Bio-Rad 1705060)

Imatinib Sensitivity

Pdgfrb$^{-/-}$ MEFs ectopically expressing either P-WT or P-Ex12 were plated in a 96-well plate, exposed to imatinib at doses ranging from 1 nM to 10 µM for 5 d, and analyzed by Cyquant (ThermoFisher Scientific C7026).

Tumor-Forming Capacity

10T1/2 fibroblasts transduced with control or experimental vectors expressing P-WT or P-Ex12 were expanded in vitro and harvested by trypsin/EDTA. Harvested cells (25×10^7) were suspended in equal parts phosphate-buffered saline and Matrigel (Corning 356237) and then implanted by subcutaneous injection into NOD-SCID mice (UTSW breeding core) with 5×10^6 cells/mouse. Tumor formation was assessed at least three times/week, and animals were euthanized by CO_2 when tumor size approached 200 mm^3 volume. Tumor specimens taken from euthanized animals were immediately bisected and either fixed in 4% paraformaldehyde or processed and FFPE sectioning or flash frozen in LN2. DNA and protein were extracted from frozen tissue using QIAGEN DNA/RNA/Protein Mini Kit.

FFPE sections were stained using hematoxylin and eosin or by immunohistochemistry for Ki67 antibody (BD Pharmigen 556003) or phospho-histone H3 antibody (EMD Millipore 06-570). Primary antibodies were detected using VectaStain Universal Quick Kit (Pk-8800).

Statistical Analyses

All quantitative analyses were carried out with two or more biological replicates and at least duplicate experiments were carried out on separate occasions. Quantitative differences were assessed using statistical tools, described in relevant figure legends.

ADDITIONAL INFORMATION

Data Deposition and Access

The *PDGFRB* variant has been submitted to ClinVar (https://www.ncbi.nlm.nih.gov/clinvar/) and can be found under accession number SCV000992360. We do not have permission to upload the raw clinical sequencing into a public repository.

Ethics Statement

The patient's legal guardian signed written informed consent and this study was approved by the institutional review board (IRB) at UT Southwestern Medical Center. Histological and molecular analyses of the human tumor specimen in this case was approved by the UT Southwestern Medical Center Institutional Review Board (protocol# STU 022013-058). Animal studies were carried out with approval of the UT Southwestern Medical Center Animal Care and Use Committee (protocol # APN-2015-101401).

Author Contributions

S.X.S., T.L., M.H., E.B., and R.W. were involved in conceptualization. D.R., A.R., T.L., L.L.Y., M.R., R.E., S.M.A., P.J.L., D.W.P., M.H., S.X.S., and R.W. were involved in data analyses. M.H., P.J.L., R.W., and Y.Z. were involved in in vivo and in vitro laboratory work. M.H., S.X.S., T.L., and E.B., were involved in writing, reviewing, and editing the manuscript.

Funding

REFERENCES

Abe A, Emi N, Tanimoto M, Terasaki H, Marunouchi T, Saito H. 1997. Fusion of the platelet-derived growth factor receptor β to a novel gene CEV14 in acute myelogenous leukemia after clonal evolution. *Blood* **90:** 4271–4277.

Agaimy A, Bieg M, Michal M, Geddert H, Märkl B, Seitz J, Moskalev EA, Schlesner M, Metzler M, Hartmann A, et al. 2017. Recurrent somatic *PDGFRB* mutations in sporadic infantile/solitary adult myofibromas but not in angioleiomyomas and myopericytomas. *Am J Surg Pathol* **41:** 195–203. doi:10.1097/PAS.0000000000000752

Alaggio R, Barisani D, Ninfo V, Rosolen A, Coffin CM. 2008. Morphologic overlap between infantile myofibromatosis and infantile fibrosarcoma: a pitfall in diagnosis. *Pediatr Dev Pathol* **11:** 355–362. doi:10.2350/07-09-0355.1

Andrae J, Gallini R, Betsholtz C. 2008. Role of platelet-derived growth factors in physiology and medicine. *Genes Dev* **22:** 1276–1312. doi:10.1101/gad.1653708

Arts FA, Chand D, Pecquet C, Velghe AI, Constantinescu S, Hallberg B, Demoulin JB. 2016. PDGFRB mutants found in patients with familial infantile myofibromatosis or overgrowth syndrome are oncogenic and sensitive to imatinib. *Oncogene* **35:** 3239–3248. doi:10.1038/onc.2015.383

Arts FA, Sciot R, Brichard B, Renard M, de Rocca Serra A, Dachy G, Noël LA, Velghe AI, Galant C, Debiec-Rychter M, et al. 2017. *PDGFRB* gain-of-function mutations in sporadic infantile myofibromatosis. *Hum Mol Genet* **26:** 1801–1810. doi:10.1093/hmg/ddx081

Azzam R, Abboud M, Muwakkit S, Khoury N, Saab R. 2009. First-line therapy of generalized infantile myofibromatosis with low-dose vinblastine and methotrexate. *Pediatr Blood Cancer* **52:** 308. doi:10.1002/pbc.21797

Chan PM, Ilangumaran S, La Rose J, Chakrabartty A, Rottapel R. 2003. Autoinhibition of the kit receptor tyrosine kinase by the cytosolic juxtamembrane region. *Mol Cell Biol* **23:** 3067–3078. doi:10.1128/MCB.23.9.3067-3078.2003

Cheung YH, Gayden T, Campeau PM, LeDuc CA, Russo D, Nguyen VH, Guo J, Qi M, Guan Y, Albrecht S, et al. 2013. A recurrent *PDGFRB* mutation causes familial infantile myofibromatosis. *Am J Hum Genet* **92:** 996–1000. doi:10.1016/j.ajhg.2013.04.026

Corbacioglu S, Kilic M, Westhoff MA, Reinhardt D, Fulda S, Debatin KM. 2006. Newly identified *c-KIT* receptor tyrosine kinase ITD in childhood AML induces ligand-independent growth and is responsive to a synergistic effect of imatinib and rapamycin. *Blood* **108:** 3504–3513. doi:10.1182/blood-2006-05-021691

Corless CL, Schroeder A, Griffith D, Town A, McGreevey L, Harrell P, Shiraga S, Bainbridge T, Morich J, Heinrich MC. 2005. *PDGFRA* mutations in gastrointestinal stromal tumors: frequency, spectrum and in vitro sensitivity to imatinib. *J Clin Oncol* **23:** 5357–5364. doi:10.1200/JCO.2005.14.068

Day M, Edwards AO, Weinberg A, Leavey PJ. 2002. Brief report: successful therapy of a patient with infantile generalized myofibromatosis. *Med Pediatr Oncol* **38:** 371–373. doi:10.1002/mpo.1350

di Tommaso A, Hagen J, Tompkins V, Muniz V, Dudakovic A, Kitzis A, Ladeveze V, Quelle DE. 2009. Residues in the alternative reading frame tumor suppressor that influence its stability and p53-independent activities. *Exp Cell Res* **315:** 1326–1335. doi:10.1016/j.yexcr.2009.01.010

Forsberg K, Valyi-Nagy I, Heldin CH, Herlyn M, Westermark B. 1993. Platelet-derived growth factor (PDGF) in oncogenesis: development of a vascular connective tissue stroma in xenotransplanted human melanoma producing PDGF-BB. *Proc Natl Acad Sci* **90:** 393–397. doi:10.1073/pnas.90.2.393

Fukasawa Y, Ishikura H, Takada A, Yokoyama S, Imamura M, Yoshiki T, Sato H. 1994. Massive apoptosis in infantile myofibromatosis. A putative mechanism of tumor regression. *Am J Pathol* **144:** 480–485.

Golub TR, Barker GF, Lovett M, Gilliland DG. 1994. Fusion of PDGF receptor β to a novel *ets*-like gene, *tel*, in chronic myelomonocytic leukemia with t(5;12) chromosomal translocation. *Cell* **77:** 307–316. doi:10.1016/0092-8674(94)90322-0

Heinrich MC, Corless CL, Demetri GD, Blanke CD, von Mehren M, Joensuu H, McGreevey LS, Chen CJ, Van den Abbeele AD, Druker BJ, et al. 2003a. Kinase mutations and imatinib response in patients with metastatic gastrointestinal stromal tumor. *J Clin Oncol* **21:** 4342–4349. doi:10.1200/JCO.2003.04.190

Heinrich MC, Corless CL, Duensing A, McGreevey L, Chen CJ, Joseph N, Singer S, Griffith DJ, Haley A, Town A, et al. 2003b. *PDGFRA* activating mutations in gastrointestinal stromal tumors. *Science* **299:** 708–710. doi:10.1126/science.1079666

Hellström M, Kalen M, Lindahl P, Abramsson A, Betsholtz C. 1999. Role of PDGF-B and PDGFR-β in recruitment of vascular smooth muscle cells and pericytes during embryonic blood vessel formation in the mouse. *Development* **126:** 3047–3055.

Hoch RV, Soriano P. 2003. Roles of PDGF in animal development. *Development* **130:** 4769–4784. doi:10.1242/dev.00721

Kamijo T, Zindy F, Roussel MF, Quelle DE, Downing JR, Ashmun RA, Grosveld G, Sherr CJ. 1997. Tumor suppression at the mouse *INK4a* locus mediated by the alternative reading frame product p19*ARF*. *Cell* **91:** 649–659. doi:10.1016/S0092-8674(00)80452-3

Kim SY, Kang JJ, Lee HH, Kang JJ, Kim B, Kim CG, Park TK, Kang H. 2011. Mechanism of activation of human c-KIT kinase by internal tandem duplications of the juxtamembrane domain and point mutations at aspartic acid 816. *Biochem Biophys Res Commun* **410:** 224–228. doi:10.1016/j.bbrc.2011.05.111

Kiyoi H, Towatari M, Yokota S, Hamaguchi M, Ohno R, Saito H, Naoe T. 1998. Internal tandem duplication of the FLT3 gene is a novel modality of elongation mutation which causes constitutive activation of the product. *Leukemia* **12:** 1333–1337. doi:10.1038/sj.leu.2401130

Kiyoi H, Ohno R, Ueda R, Saito H, Naoe T. 2002. Mechanism of constitutive activation of FLT3 with internal tandem duplication in the juxtamembrane domain. *Oncogene* **21:** 2555–2563. doi:10.1038/sj.onc.1205332

Laetsch TW, DuBois SG, Mascarenhas L, Turpin B, Federman N, Albert CM, Nagasubramanian R, Davis JL, Rudzinski E, Feraco AM, et al. 2018. Larotrectinib for paediatric solid tumours harbouring *NTRK* gene fusions: phase 1 results from a multicentre, open-label, phase 1/2 study. *Lancet Oncol* **19:** 705–714. doi:10.1016/S1470-2045(18)30119-0

Liang L, Yan XE, Yin Y, Yun CH. 2016. Structural and biochemical studies of the PDGFRA kinase domain. *Biochem Biophys Res Commun* **477:** 667–672. doi:10.1016/j.bbrc.2016.06.117

Linhares ND, Freire MC, Cardenas RG, Bahia M, Puzenat E, Aubin F, Pena SD. 2014. Modulation of expressivity in PDGFRB-related infantile myofibromatosis: a role for PTPRG? *Genet Mol Res* **13:** 6287–6292. doi:10.4238/2014.August.15.11

Magnusson MK, Meade KE, Brown KE, Arthur DC, Krueger LA, Barrett AJ, Dunbar CE. 2001. Rabaptin-5 is a novel fusion partner to platelet-derived growth factor β receptor in chronic myelomonocytic leukemia. *Blood* **98:** 2518–2525. doi:10.1182/blood.V98.8.2518

Martignetti JA, Tian L, Li D, Ramirez MC, Camacho-Vanegas O, Camacho SC, Guo Y, Zand DJ, Bernstein AM, Masur SK, et al. 2013. Mutations in *PDGFRB* cause autosomal-dominant infantile myofibromatosis. *Am J Hum Genet* **92:** 1001–1007. doi:10.1016/j.ajhg.2013.04.024

Mashiah J, Hadj-Rabia S, Dompmartin A, Harroche A, Laloum-Grynberg E, Wolter M, Amoric JC, Hamel-Teillac D, Guero S, Fraitag S, et al. 2014. Infantile myofibromatosis: a series of 28 cases. *J Am Acad Dermatol* **71:** 264–270. doi:10.1016/j.jaad.2014.03.035

McArthur GA. 2006. Dermatofibrosarcoma protuberans: a surgical disease with a molecular savior. *Curr Opin Oncol* **18:** 341–346. doi:10.1097/01.cco.0000228739.62756.df

Mudry P, Slaby O, Neradil J, Soukalova J, Melicharkova K, Rohleder O, Jezova M, Seehofnerova A, Michu E, Veselska R, et al. 2017. Case report: rapid and durable response to PDGFR targeted therapy in a child with refractory multiple infantile myofibromatosis and a heterozygous germline mutation of the *PDGFRB* gene. *BMC Cancer* **17:** 119. doi:10.1186/s12885-017-3115-x

Murray N, Hanna B, Graf N, Fu H, Mylène V, Campeau PM, Ronan A. 2017. The spectrum of infantile myofibromatosis includes both non-penetrance and adult recurrence. *Eur J Med Genet* **60:** 353–358. doi:10.1016/j.ejmg.2017.02.005

Pardee AB. 1989. G1 events and regulation of cell proliferation. *Science* **246:** 603–608. doi:10.1126/science.2683075

Parham DM. 2018. Fibroblastic and myofibroblastic tumors of children: new genetic entities and new ancillary testing. *F1000Res* **7:** F1000. doi:10.12688/f1000research.16236.1

Peng B, Hayes M, Resta D, Racine-Poon A, Druker BJ, Talpaz M, Sawyers CL, Rosamilia M, Ford J, Lloyd P, et al. 2004. Pharmacokinetics and pharmacodynamics of imatinib in a phase I trial with chronic myeloid leukemia patients. *J Clin Oncol* **22:** 935–942. doi:10.1200/JCO.2004.03.050

Pond D, Arts FA, Mendelsohn NJ, Demoulin JB, Scharer G, Messinger Y. 2018. A patient with germ-line gain-of-function *PDGFRB* p.N666H mutation and marked clinical response to imatinib. *Genet Med* **20:** 142–150. doi:10.1038/gim.2017.104

Reindl C, Bagrintseva K, Vempati S, Schnittger S, Ellwart JW, Wenig K, Hopfner KP, Hiddemann W, Spiekermann K. 2006. Point mutations in the juxtamembrane domain of FLT3 define a new class of activating mutations in AML. *Blood* **107:** 3700–3707. doi:10.1182/blood-2005-06-2596

Reznikoff CA, Brankow DW, Heidelberger C. 1973. Establishment and characterization of a cloned line of C3H mouse embryo cells sensitive to postconfluence inhibition of division. *Cancer Res* **33:** 3231–3238.

Short NJ, Kantarjian H, Ravandi F, Daver N. 2019. Emerging treatment paradigms with FLT3 inhibitors in acute myeloid leukemia. *Ther Adv Hematol* **10:** 2040620719827310. doi:10.1177/2040620719827310

Silva RL, Thornton JD, Martin AC, Rehg JE, Bertwistle D, Zindy F, Skapek SX. 2005. *Arf*-dependent regulation of Pdgf signaling in perivascular cells in the developing mouse eye. *EMBO J* **24:** 2803–2814. doi:10.1038/sj.emboj.7600751

Soriano P. 1994. Abnormal kidney development and hematological disorders in PDGF β-receptor mutant mice. *Genes Dev* **8:** 1888–1896. doi:10.1101/gad.8.16.1888

Sramek M, Neradil J, Macigova P, Mudry P, Polaskova K, Slaby O, Noskova H, Sterba J, Veselska R. 2018. Effects of sunitinib and other kinase inhibitors on cells harboring a *PDGFRB* mutation associated with infantile myofibromatosis. *Int J Mol Sci* **19:** E2599. doi:10.3390/ijms19092599

Stover EH, Chen J, Folens C, Lee BH, Mentens N, Marynen P, Williams IR, Gilliland DG, Cools J. 2006. Activation of FIP1L1-PDGFRα requires disruption of the juxtamembrane domain of PDGFRα and is FIP1L1-independent. *Proc Natl Acad Sci* **103:** 8078–8083. doi:10.1073/pnas.0601192103

Tallquist M, Kazlauskas A. 2004. PDGF signaling in cells and mice. *Cytokine Growth Factor Rev* **15:** 205–213. doi:10.1016/j.cytogfr.2004.03.003

Toffalini F, Demoulin JB. 2010. New insights into the mechanisms of hematopoietic cell transformation by activated receptor tyrosine kinases. *Blood* **116:** 2429–2437. doi:10.1182/blood-2010-04-279752

Wang J, Hisaoka M, Shimajiri S, Morimitsu Y, Hashimoto H. 1999. Detection of COL1A1-PDGFB fusion transcripts in dermatofibrosarcoma protuberans by reverse transcription-polymerase chain reaction using archival formalin-fixed, paraffin-embedded tissues. *Diagn Mol Pathol* **8:** 113–119. doi:10.1097/00019606-199909000-00002

Weaver MS, Navid F, Huppmann A, Meany H, Angiolillo A. 2015. Vincristine and dactinomycin in infantile myofibromatosis with a review of treatment options. *J Pediatr Hematol Oncol* **37:** 237–241. doi:10.1097/MPH.0000000000000286

Widau RC, Zheng Y, Sung CY, Zelivianskaia A, Roach LE, Bachmeyer KM, Abramova T, Desgardin A, Rosner A, Cunningham JM, et al. 2012. p19[Arf] represses platelet-derived growth factor receptor β by transcriptional and posttranscriptional mechanisms. *Mol Cell Biol* **32:** 4270–4282. doi:10.1128/MCB.06424-11

Wiswell TE, Davis J, Cunningham BE, Solenberger R, Thomas PJ. 1988. Infantile myofibromatosis: the most common fibrous tumor of infancy. *J Pediatr Surg* **23:** 315–318. doi:10.1016/S0022-3468(88)80196-9

Wu SY, McCavit TL, Cederberg K, Galindo RL, Leavey PJ. 2015. Chemotherapy for generalized infantile myofibromatosis with visceral involvement. *J Pediatr Hematol Oncol* **37:** 402–405. doi:10.1097/MPH.0000000000000132